Weierstraß-Institut
für Angewandte Analysis und Stochastik

Leibniz-Institut im Forschungsverbund Berlin e. V.

Preprint ISSN 2198-5855

Unusual ways of four-wave mixing instability

Shalva Amiranashvili, Uwe Bandelow

submitted: April 28, 2022

Weierstrass Institute
Mohrenstr. 39
10117 Berlin
Germany
E-Mail: shalva.amiranashvili@wias-berlin.de
uwe.bandelow@wias-berlin.de

No. 2934
Berlin 2022

2020 *Mathematics Subject Classification.* 78A40, 78A60.

2010 *Physics and Astronomy Classification Scheme.* 42.25.Bs, 42.65.Sf, 42.65.Wi, 42.81.Dp.

Key words and phrases. Nonlinear fibers, modulation instability, four wave mixing instability, Lighthill criterion, negative frequencies.

Edited by
Weierstraß-Institut für Angewandte Analysis und Stochastik (WIAS)
Leibniz-Institut im Forschungsverbund Berlin e. V.
Mohrenstraße 39
10117 Berlin
Germany

Fax: +49 30 20372-303
E-Mail: preprint@wias-berlin.de
World Wide Web: http://www.wias-berlin.de/

Unusual ways of four-wave mixing instability

Shalva Amiranashvili, Uwe Bandelow

Abstract

A pump carrier wave in a dispersive system may decay by giving birth to blue- and red-shifted satellite waves due to modulation or four-wave mixing instability. We analyse situations where the satellites are so different from the carrier wave, that the red-shifted satellite either changes its propagation direction ($k < 0, \omega > 0$) or even gets a negative frequency ($k, \omega < 0$). Both situations are beyond the envelope approach and require application of Maxwell equations.

1 Introduction

The key property of a dispersive system is the existence of linear small-amplitude waves, e.g., of the form $\mathrm{Re}\left[e^{i(\mathbf{kr}-\omega t)}\right]$ with a certain dispersion relation $\omega = \ell(\mathbf{k})$. An increase of power results in a nonlinear wave, which may become unstable [1]. A very common instability scenario is excitation of two growing satellite waves with the reduced and increased frequencies: the Stokes and anti-Stokes (or just red/blue-shifted) spectral lines [2]. The satellite frequencies are equally displaced from the incident one. Starting from the seminal study on modulated water waves [3], the effect was observed in many nonlinear dispersive systems including optical fibers [4], which are in the focus of this work.

A small frequency displacement that is proportional to the incident power is the defining feature of the most common modulation instability (MI). If the new lines are separated from the carrier, no matter how small the incident power, one deals with a four-wave mixing (FWM) instability. In both cases, the parameters of the blue-shifted (b) and red-shifted (r) satellites are connected to that of the carrier (c) wave by the resonance (phase matching) conditions

$$\omega_b + \omega_r = 2\omega_c, \quad \mathbf{k}_b + \mathbf{k}_r = 2\mathbf{k}_c, \tag{1}$$

where the dispersion relation $\omega = \ell(\mathbf{k})$ must hold for all three waves [5, 6].

Conditions (1) are necessary but not sufficient, the sufficient condition for MI was given by Lighthill [7]. With respect to optical fibers, both instability scenarios are described by a generalized nonlinear Schrödinger equation (GNLSE) for the wave envelope [8, 9, 10, 11, 12, 13, 14, 15]. Moreover, Lighthill's criterion can be reformulated to cover both MI and FWM regimes [16]. Note that GNLSE actually refers to a class of increasingly complex equations with higher-order dispersion, losses, Raman integral, and self-steepening derivative terms [17, 18, 19, 20, 21, 22, 23, 24]. To our knowledge, the most comprehensive "all included" MI analysis was published in [15]. One can also study MI directly with the full Maxwell equations [25].

This work considers wave instabilities in optical fibers and takes advantage of the fact that fiber dispersion can be engineered [26]. One can manipulate $\ell(\mathbf{k})$ and solutions of the system (1) to excite a wide range of frequencies via the FWM mechanism [27, 28, 29, 30, 31]. We aim to answer the question: can the red-shifted satellite be so different from the carrier wave that it *either propagates in the opposite direction or gets a negative frequency*, as schematically shown in Fig. 1? In this case, the blue-shifted frequency will be greater than $2\omega_c$.

Appearance of the backward wave may resemble the Brillouin scattering with the difference that the FWM instability takes place due to cubic nonlinearities and without any contribution of material waves. Our interest to negative frequencies is motivated by recent papers on classical nonlinear optics (and

DOI 10.20347/WIAS.PREPRINT.2934 Berlin 2022

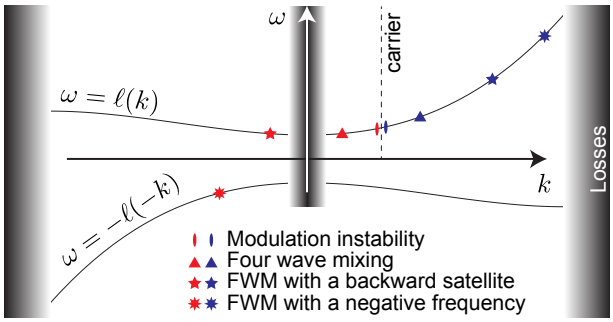

Figure 1: A schematic dispersion law within a transparency window and possible instability regimes are shown. An anisotropic $\ell(\mathbf{k})$ with $\mathbf{k} = (0, 0, k)$ is used for better visibility. The necessary Eq. (1) selects the feasible instability. A sufficient condition (e.g., that of Lighthill) decides whether the instability develops or not.

on water waves [32, 33]), where calculation of the excited spectral line leads to a negative frequency. One scenario is scattering of a wave packet at a quickly moving perturbation of the refractive index created by another pulse. One can observe several scattered waves: a standard frequency-shifted backward wave identical to that reflected by a moving mirror [34], forward scattering [35], and an exotic classical Hawking radiation with a negative frequency [36, 37]. Another option is the so-called dispersive or Cherenkov radiation emitted by solitons in fibers [38]. A formal calculation of the radiation frequency may lead to a negative value. The positive-frequency partner of the emitted wave was observed in experiment [39, 40] and predicted by a novel modification of GNLSE [41, 42]. A search for new phenomena involving negative frequencies seems to be interesting and instructive; the stability problem for a nonlinear wave is worth a try.

2 Framework

The majority of studies on MI and FWM instability in optical fibers use various versions of GNLSE. The latter is extremely powerful and can be adapted to describe the contribution of negative frequencies [41, 42]. Yet, GNLSE does not fit well to our needs for several reasons. *First*, it describes waves moving in one direction, a possible backward satellite is not covered. *Second*, GNLSE approximates medium dispersion by Taylor expansion around a carrier frequency. The expansion is limited by its convergence radius, which is determined by resonances of the dielectric function $\epsilon(\omega, \mathbf{k})$ in the complex ω-plane. If the low-frequency resonances are present, the Taylor expansion at ω_c covers neither the red stars in Fig. 1 nor the general relation [43]

$$\epsilon^*(\omega, \mathbf{k}) = \epsilon(-\omega^*, -\mathbf{k}), \tag{2}$$

which we will use later. *Third*, GNLSE in optical fibers is a space-propagated problem in (t, z) coordinate space. The initial pulse is given for some z and $\forall t$, in conflict with the causality principle. The pulse shape is then calculated for a larger z and $\forall t$. Dealing with such a delicate question as negative frequencies, it is preferable to have a causal system that evolves in time.

For these reasons, we will follow [25] and directly employ Maxwell equations to study the stability problem with the difference being that our system is time-propagated and retains causality. Before proceeding, we need to make a few remarks.

- Given a reasonable incident power, MI satellites are too close to the carrier to have unusual

properties. FWM instability is the only case of interest.

- Plane waves in what follows will have a real $\mathbf{k}$ and possibly complex ω, which is called "negative" if $\mathrm{Re}(\omega) < 0$. We should modify Eq. (1) for $\omega \in \mathbb{C}$.
- $\mathrm{Re}\left[e^{i(\mathbf{kr}-\omega t)}\right]$ is invariant with respect to the substitution $\omega \mapsto -\omega^*$, $\mathbf{k} \mapsto -\mathbf{k}$, generated by the complex conjugation, cf. Eq. (2).
- Any positive-frequency branch of the dispersion law has a negative-frequency partner

$$\omega = \ell(\mathbf{k}) \quad \text{comes with} \quad \omega = -\ell^*(-\mathbf{k}). \tag{3}$$

The situation we are interested in is schematically shown in Fig. 1 by red stars. Now we can formulate the problem more precisely. Let ω_c, $\mathbf{k}_c$ and ω_b, $\mathbf{k}_b$ belong to the positive-frequency branch in Eq. (3). It is not enough to know whether ω_r, $\mathbf{k}_r$, which come from Eq. (1), can belong to either backward or negative-frequency branch. We shall get a dispersion relation for the satellites and study if they grow up.

3 Model equation

A generic electromagnetic wave is described by the wave equation

$$\mu_0 \partial_t^2 \mathbf{D} + \mathrm{rot}\,\mathrm{rot}\,\mathbf{E} = 0, \tag{4}$$

where the displacement $\mathbf{D}(t,\mathbf{r})$ and field $\mathbf{E}(t,\mathbf{r})$ are confined by a material relation. We consider an isotropic dispersive dielectric medium with a cubic nonlinearity that is characterized by a single Kerr parameter χ

$$\frac{1}{\epsilon_0}\mathbf{D} = \mathbf{E} + K \circ \mathbf{E} + \chi|\mathbf{E}|^2\mathbf{E}, \tag{5}$$

where, for simplicity, χ is just a constant. The simplest non-dispersive nonlinearity is combined with a generic linear dispersion: the term $K \circ \mathbf{E}$ denotes a causal convolution with a suitable kernel $K(t,\mathbf{r})$

$$K \circ \mathbf{E} = \int_0^\infty \int_{\mathbb{R}^3} K(t',\mathbf{r}')\mathbf{E}(t-t',\mathbf{r}-\mathbf{r}')dt'd^3\mathbf{r}'.$$

A wave with $\mathbf{E} \propto e^{i(\mathbf{kr}-\omega t)}$ yields $K \circ \mathbf{E} = (\epsilon - 1)\mathbf{E}$, where the dielectric function reads [43]

$$\epsilon(\omega,\mathbf{k}) = 1 + \int_0^\infty \int_{\mathbb{R}^3} K(t,\mathbf{r})e^{i(\omega t-\mathbf{kr})}dtd^3\mathbf{r}. \tag{6}$$

Again, for simplicity and with optical fibers in mind, we consider only 1D propagation with

$$\mathbf{k} = (0,0,k), \quad \mathbf{E} = \mathbf{E}(t,z) = (E_x, E_y, 0),$$

and use the notations

$$\epsilon(\omega,k) = \epsilon(\omega,\mathbf{k})|_{\mathbf{k}=(0,0,k)}, \quad \ell(k) = \ell(\mathbf{k})|_{\mathbf{k}=(0,0,k)}.$$

Equations (4) and (5) are then reduced to a single partial differential equation (PDE) for a complex variable Ψ

$$\partial_t^2\left(\Psi + K \circ \Psi + \chi|\Psi|^2\Psi\right) - c^2\partial_z^2\Psi = 0, \tag{7}$$

where $\Psi(t,z) = E_x + iE_y$.

Equation (7) is our starting point. It might look like an envelope equation, but it applies directly to the electric field. Being an exact reduction of (4–5), it is not limited by any kind of unidirectional or slowly-varying-envelope approximation. Moreover, Eq. (7) describes causal evolution of both forward and backward waves for an arbitrary medium dispersion. Both positive and negative frequencies are covered such that Eq. (7) is well suited to study two unusual FWM scenarios from Fig. 1.

4 Carrier wave

For brevity we introduce a kind of generalized dispersion function $\mathfrak{E}(\omega,k)$ and notations for its derivatives

$$\mathfrak{E} = \epsilon(\omega,k) - \frac{k^2c^2}{\omega^2}, \quad \dot{\mathfrak{E}} = \frac{\partial\mathfrak{E}}{\partial\omega}, \quad \mathfrak{E}' = \frac{\partial\mathfrak{E}}{\partial k}. \tag{8}$$

A small-amplitude $Ae^{i(kz-\omega t)}$ solution to Eq. (7) corresponds to a circular linear wave and requires $\mathfrak{E}(\omega,k)=0$. This yields the main (generally speaking, multivalued) dispersion relation $\omega=\ell(k)$ and its partner (3). The group velocity V and the group velocity dispersion D are given by the derivatives of an implicit function

$$V = \frac{d\omega}{dk} = -\frac{\mathfrak{E}'}{\dot{\mathfrak{E}}}, \tag{9}$$

$$D = \frac{d^2\omega}{dk^2} = -\frac{\ddot{\mathfrak{E}}V^2 + 2\dot{\mathfrak{E}}'V + \mathfrak{E}''}{\dot{\mathfrak{E}}}, \tag{10}$$

where a bit clumsy form of $D(\omega,k)$ is the price we pay for a general $\epsilon(\omega,k)$.

A possible instability develops upon a weakly nonlinear circular carrier wave

$$\Psi = A_c e^{i(k_c z-\omega_c t)} \quad \text{with} \quad \sigma = \chi A_c^2 \ll 1, \tag{11}$$

where σ is a dimensionless power parameter. The carrier should belong to a transparency domain, such that $\omega_c, k_c \in \mathbb{R}$ and $\mathrm{Im}[\epsilon(\omega_c,k_c)] \approx 0$. Equations (7) and (11) yield a nonlinear dispersion relation

$$\mathfrak{E}(\omega_c,k_c) + \sigma = 0. \tag{12}$$

The carrier wave has a nonlinear frequency shift ω_{nl}, which is defined such that $\omega_c - \omega_{\mathsf{nl}}$ and k_c satisfy the linear dispersion relation $\mathfrak{E}(\omega_c-\omega_{\mathsf{nl}},k_c)=0$, i.e.,

$$\omega_{\mathsf{nl}} = -\frac{\sigma}{\dot{\mathfrak{E}}_c} + O(\sigma^2). \tag{13}$$

Here and from now on, we use the notations

$$\mathfrak{E}_\xi,\ \dot{\mathfrak{E}}_\xi,\ \mathfrak{E}'_\xi,\ V_\xi,\ D_\xi,$$

when the involved quantities are calculated for the carrier wave ($\xi=c$) or its satellites ($\xi=b,r$). We now turn to the carrier stability problem.

5 Dispersion relation

We consider a small perturbation ψ of the carrier wave (11)

$$\Psi(t,z) = A_c e^{i(k_c z - \omega_c t)} + \psi(t,z),$$

which is subject to a linear PDE yielded by Eq. (7)

$$\partial_t^2 \left(\psi + K \circ \psi + 2\sigma\psi + \sigma e^{2i(k_c z - \omega_c t)}\psi^*\right) - c^2 \partial_z^2 \psi = 0.$$

We look for a special solution for ψ that combines one blue- and one red-shifted satellite

$$\psi = A_b e^{i(k_b z - \omega_b t)} + A_r e^{i(k_r z - \omega_r t)},$$

with $A_{b,r} = \text{const}$. Recall that ω_c and all wavevectors are real. The satellite frequencies ω_b and ω_r may be real or complex. By construction we require, cf. Eq. (1),

$$\omega_b + \omega_r^* = 2\omega_c \quad \text{and} \quad k_b + k_r = 2k_c, \tag{14}$$

such that the non-homogeneous term in the PDE for ψ is expressed through the same satellites

$$e^{2i(k_c z - \omega_c t)}\psi^* = A_r^* e^{i(k_b z - \omega_b t)} + A_b^* e^{i(k_r z - \omega_r t)}.$$

The amplitudes A_b and A_r are then non-trivial solutions to a system of two linear homogeneous equations

$$\begin{pmatrix} \mathfrak{E}_b + 2\sigma & \sigma \\ \sigma & \mathfrak{E}_r^* + 2\sigma \end{pmatrix} \begin{pmatrix} A_b \\ A_r^* \end{pmatrix} = \begin{pmatrix} 0 \\ 0 \end{pmatrix}, \tag{15}$$

which finally leaves us with the dispersion relation for the satellites

$$(\mathfrak{E}_b + 2\sigma)(\mathfrak{E}_r^* + 2\sigma) = \sigma^2. \tag{16}$$

Equation (16), being *causal and valid for positive and negative frequencies*, contains all we need to know about the instability regimes depicted in Fig. 1.

Let us make a few remarks before continuing. Figure 1 and the standard phase matching conditions (1) apply, of course, to the real parts of the satellite frequencies. The satellites will typically belong to the transparency window, and yet $\omega_{b,r}$ may be complex which indicates instability. If it is the case, $\mathfrak{E}_b$ and $\mathfrak{E}_r$ are complex as well and the complex conjugation in Eq. (16) is essential. Equations (2) and (14) yield that

$$\mathfrak{E}_r^* = \mathfrak{E}(-\omega_r^*, -k_r) = \mathfrak{E}(\omega_b - 2\omega_c, k_b - 2k_c), \tag{17}$$

such that all stable solutions of Eq. (16) can be plotted as a real-valued $\omega_b(k_b)$. The plot contains gaps, where $\omega_b(k_b)$ turns complex because of losses or instability.

It is remarkable that the merged MI/FWM problem gets such a compact formulation as Eq. (16) for an arbitrary $\epsilon(\omega, k)$. On the other hand, the dispersion relation for the satellites that comes from a GNLSE can be solved immediately [8, 9, 10, 11, 12, 13, 14, 15]. At most, one is facing a fourth-order equation [25]. In our case, the implicit Eq. (16) requires aditional work to be done (Fig. 2).

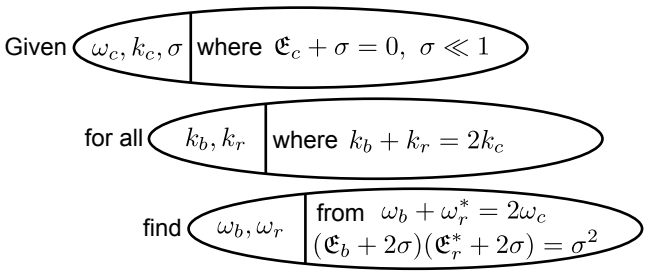

Figure 2: Informal summary of the dispersion relation (16) for the satellites. Complex values of $\omega_{b,r}$ indicate instability, $\mathfrak{E}_\xi$ denotes $\epsilon(\omega_\xi, k_\xi) - k_\xi^2 c^2/\omega_\xi^2$ with $\xi = c, b, r$.

6 MI case

The general approach of the previous sections is an overkill for the classical MI, where the carrier wave and both its satellites perfectly fit to a slowly varying envelope approximation and GNLSE. Nevertheless, MI is of course covered by Eq. (16). Note that for $k_{b,r} = k_c$, we have an exact solution $\omega_{b,r} = \omega_c$ of the problem sketched in Fig. 2. In the vicinity of this solution, one can set

$$\omega_b = \omega_c + \Omega, \quad \omega_r = \omega_c - \Omega^*, \quad k_{b,r} = k_c \pm \kappa,$$

such that both phase matching conditions (14) are satisfied, and look for $\Omega(\kappa)$. We expand Eq. (16) with respect to Ω and κ. Two successive iterations yield the classical result

$$(\Omega - \kappa V_c)^2 = \left(2\omega_{\mathsf{nl}} + \frac{D_c\kappa^2}{2}\right)\frac{D_c\kappa^2}{2}, \tag{18}$$

which contains the group velocity (9) and group velocity dispersion (10) of the carrier wave. The nonlinear frequency shift ω_{nl} was defined in Eq. (13).

For (Lighthill criterion) $\omega_{\mathsf{nl}} D_c < 0$, Eq. (18) describes MI that evolves in time with the complex modulation frequency Ω and the maximal increment

$$[\operatorname{Im}\Omega]_{\mathsf{max}} = |\omega_{\mathsf{nl}}| = \frac{\sigma}{|\dot{\mathfrak{E}}_c|}. \tag{19}$$

Note, that a more common MI formulation for fibers is space-propagated and yields complex $\kappa(\Omega)$, see [44].

7 FWM case

We are now ready to consider the FWM instability without any reference to GNLSE and dispersion coefficients at carrier frequency. Let us neglect for a moment the right-hand-side of Eq. (16)

$$\big[\mathfrak{E}(\omega_b, k_b) + 2\sigma\big]\big[\mathfrak{E}^*(\omega_r, k_r) + 2\sigma\big] = 0. \tag{20}$$

Solutions of Eq. (20) are split into the "blue" and "red" ones. Within the transparency domain, we get two real-valued implicit functions, which can be plotted on the same (k_b, ω_b) plane using Eq. (17). An example is shown in Fig. 3a. Assume that these two curves cross each other at some point (k_{b0}, ω_{b0}), see the inset in Fig. 3a. In the vicinity of this double root one can set

$$\begin{aligned} &\omega_b = \omega_{b0} + \Omega, && \omega_r = \omega_{r0} - \Omega^*, && \Omega = O(\sigma), \\ &k_r = k_{b0} + \kappa, && k_r = k_{r0} - \kappa, && \kappa = O(\sigma), \end{aligned}$$

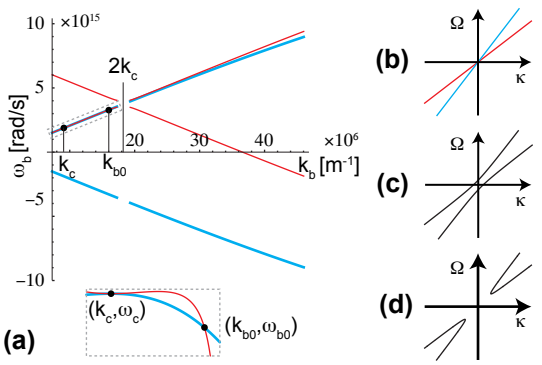

Figure 3: (a) Both blue and red solutions of Eq. (20) are plotted as $\omega_b(k_b)$ for $k_b \geq k_c$. We use a bulk fused silica dispersion function [45], take the carrier wave at 1μm, and set $\sigma = 0$. A gap for $\omega_b \approx 2k_c$ (i.e., $\omega_r \approx 0$) appears due to the low-frequency absorption of the red satellite. The FWM instability results from a generic crossing of the red and blue curves on the inset. Panels (b,c,d) show stable and unstable reconnections yielded by the right-hand-side of the full Eq. (16).

with $\omega_{r0} = 2\omega_c - \omega_{b0},\ k_{r0} = 2k_c - k_{b0}$ and expand

$$\mathfrak{E}_b = -2\sigma + \dot{\mathfrak{E}}_{b0}\Omega + \mathfrak{E}'_{b0}\kappa + O(\sigma^2),$$
$$\mathfrak{E}_r = -2\sigma - \dot{\mathfrak{E}}_{r0}\Omega^* - \mathfrak{E}'_{r0}\kappa + O(\sigma^2),$$

where the derivatives $\dot{\mathfrak{E}}_{b0,r0}$ and $\mathfrak{E}'_{b0,r0}$ and the corresponding group velocities $V_{b0,r0}$ are real.

We now return to the full Eq. (16), consider the vicinity of the intersection point, and derive

$$(\Omega - V_{b0}\kappa)(\Omega - V_{r0}\kappa) = -\frac{\sigma^2}{\dot{\mathfrak{E}}_{b0}\dot{\mathfrak{E}}_{r0}}. \tag{21}$$

The effect of the right-hand-side is that the two lines $\Omega = V_{b0}\kappa$ and $\Omega = V_{r0}\kappa$ (Fig. 3b) are now reconnected in one of two possible ways, as shown in Fig. 3c,d. A gap, like one in Fig. 3d, indicates a complex-valued $\Omega(\kappa)$ and results in the FWM instability. The latter occurs if

$$\dot{\mathfrak{E}}_{b0}\dot{\mathfrak{E}}_{r0} > 0, \tag{22}$$

and develops with the maximal increment

$$[\mathrm{Im}\,\Omega]_{\mathsf{max}} = \frac{\sigma}{\sqrt{\dot{\mathfrak{E}}_{b0}\dot{\mathfrak{E}}_{r0}}}. \tag{23}$$

It is remarkable that the MI increment (19) is covered by Eq. (23) for $\omega_{b0} = \omega_{r0} = \omega_c$. Equation (23) is universal. On the other hand, Eq. (22) is very different from the MI criterion because it does not depend on the nonlinear frequency shift.

8 Examples

To summarise the previous section: an unusual scenario of the FWM instability occurs if an intersection of two curves yielded by Eq. (20), like (k_{b0}, ω_{b0}) in the inset in Fig. 3a, takes place not before but after the attenuation gap at $2k_c$, in which case the red-shifted wave-vector $k_{r0} = 2k_c - k_{b0}$ is negative.

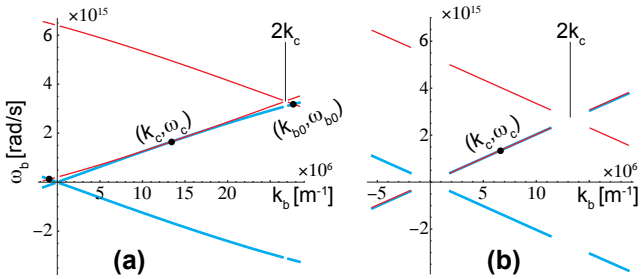

Figure 4: Solutions of the reduced Eq. (20) are shown for (a) KSR-5 glass with the carrier wave at $1.14\,\mu$m and (b) ZBLAN with the carrier wave at $1.4\,\mu$m. Change to the full Eq. (16) yields the FWM instability with the backward satellite but not the negative-frequency wave.

Two cases are then possible. A positive value of $\omega_{r0} = 2\omega_c - \omega_{b0}$ means a back-propagating satellite, otherwise one deals with a forward negative-frequency wave.

An example of the backward propagating red satellite is shown in Fig. 4a for KRS-5 glass [45], which is transparent from 0.6–$40\,\mu$m, and for a carrier at $1.14\,\mu$m. The backward satellite is at $15.6\,\mu$m. Similar behavior is expected in several other materials.

FWM instability at a negative frequency is a different story: typical dispersive materials from [45] proved to be unsuitable. Some systems are very close to the required behaviour (e.g., ZBLAN with the carrier wave at $1.4\,\mu$m in Fig. 4b) because the red and blue curves are very close to each other. Double roots with negative frequencies should appear for a slightly tuned dispersion law. However, one can demonstrate that even in such a favourable case the negative-frequency wave is not generated because the instability condition (22) is not satisfied. To demonstrate this, we use Eq. (9) to rewrite the inequality (22) as $(\mathfrak{E}'_{b0}/V_{b0})(\mathfrak{E}'_{r0}/V_{r0}) > 0$. As spatial dispersion is small for optical materials, Eq. (8) yields that $\mathfrak{E}' \approx -2kc^2/\omega^2$ and the FWM instability criterion takes the form

$$(k_{b0}/V_{b0})(k_{r0}/V_{r0}) > 0. \tag{24}$$

Examining Fig. 1, we see that inequality (24) is satisfied for the backward satellite but not for the negative-frequency one.

9 Conclusions

Nonlinear waves in dispersive systems are typically decomposed giving birth to new satellite waves, but how far these satellites can go from their origin? Can they go beyond the standard slowly varying envelope approximation and even beyond an extended envelope equation equipped by numerous dispersion coefficients? To address these questions we studied the carrier stability problem using a general material relation (5) and an exact reduction (7) of Maxwell equations. The dielectric function is not expanded at carrier frequency, moreover, the system in question evolves in time in full agreement with the causality principle. This approach resulted in a surprisingly compact dispersion relation for the satellite frequencies (16), which however is implicit and difficult to analyse, as compared to the standard space-propagated modelling of the optical four-wave instabilities. Using geometrical arguments, we revealed the instability criterion (22), and a general expression (23) for the instability increment. In the first place, we have found that the red-shifted satellite can reverse its velocity in the lab frame and propagate backward to the carrier, as long as the dispersive material is transparent for the infrared radiation. In the second place, we have found that generation of the negative-frequency satellite, while

formally possible, does not take place because the wave-mixing instability is switched off for this exotic wave.

References

[1] G. B. Whitham. *Linear and nonlinear waves*. John Wiley & Sons, 1974.

[2] V. E. Zakharov and L. A. Ostrovsky. Modulation instability: the beginning. *Physica D: Nonlinear Phenomena*, 238(5):540–548, March 2009.

[3] T. B. Benjamin and J. E. Feir. The disintegration of wave trains on deep water Part 1. Theory. *J. Fluid Mech.*, 27(3):417–430, February 1967.

[4] K. Tai, A. Hasegawa, and A. Tomita. Observation of modulational instability in optical fibers. *Phys. Rev. Lett.*, 56(2):135–138, January 1986.

[5] C. Lin, W. A. Reed, A. D. Pearson, and H.-T. Shang. Phase matching in the minimum-chromatic-dispersion region of single-mode fibers for stimulated four-photon mixing. *Opt. Lett.*, 6(10):493–495, October 1981.

[6] S. J. Garth and C. Pask. Four-photon mixing and dispersion in single-mode fibers. *Opt. Lett.*, 11(6):380–382, June 1986.

[7] M. J. Lighthill. Contributions to the theory of waves in non-linear dispersive systems. *IMA Journal of Applied Mathematics*, 1(3):269–306, 1965.

[8] S. B. Cavalcanti, J. C. Cressoni, H. R. da Cruz, and A. S. Gouveia-Neto. Modulation instability in the region of minimum group-velocity dispersion of single-mode optical fibers via an extended nonlinear Schrödinger equation. *Phys. Rev. A*, 43(11):6162–6165, June 1991.

[9] F. Kh. Abdullaev, S. A. Darmanyan, S. Bischoff, P. L. Christiansen, and M. P Sørensen. Modulational instability in optical fibers near the zero dispersion point. *Opt. Commun.*, 108(1–3):60–64, May 1994.

[10] M. Yu, C. J. McKinstrie, and G. P. Agrawal. Modulational instabilities in dispersion-flattened fibers. *Phys. Rev. E*, 52(1):1072–1080, July 1995.

[11] A. Demircan and U. Bandelow. Supercontinuum generation by the modulation instability. *Opt. Commun.*, 244(1):181–185, 2005.

[12] A. Demircan and U. Bandelow. Analysis of the interplay between soliton fission and modulation instability in supercontinuum generation. *Appl. Phys. B*, 86(1):31–39, 2007.

[13] S. Kumar, R. Herrero, M. Botey, and K. Staliunas. Taming of modulation instability by spatio-temporal modulation of the potential. *Sci. Rep.*, 5(13268), August 2015.

[14] A. Chabchoub, B. Kibler, C. Finot, G. Millot, M. Onorato, J. M. Dudley, and A. V. Babanin. The nonlinear Schrödinger equation and the propagation of weakly nonlinear waves in optical fibers and on the water surface. *Annals of Physics*, 361:490–500, October 2015.

[15] P. Béjot, B. Kibler, E. Hertz, B. Lavorel, and O. Faucher. General approach to spatiotemporal modulational instability processes. *Phys. Rev. A*, 83(1):013830, January 2011.

[16] Sh. Amiranashvili and E. Tobisch. Extended criterion for the modulation instability. *New J. Phys.*, 21(3):033029, March 2019.

[17] K. J. Blow and D. Wood. Theoretical description of transient stimulated Raman scattering in optical fibers. *IEEE J. Quantum Electron.*, 25(15):2665–2673, 1989.

[18] T. Brabec and F. Krausz. Nonlinear optical pulse propagation in the single-cycle regime. *Phys. Rev. Lett.*, 78(17):3282–3285, 1997.

[19] A. V. Husakou and J. Herrmann. Supercontinuum generation of higher-order solitons by fission in photonic crystal fibers. *Phys. Rev. Lett.*, 87(20):203901, 2001.

[20] M. Kolesik, J. V. Moloney, and M. Mlejnek. Unidirectional optical pulse propagation equation. *Phys. Rev. Lett.*, 89(28):283902, 2002.

[21] P. Kinsler and G. H. C. New. Few-cycle pulse propagation. *Phys. Rev. A*, 67(2):023813, 2003.

[22] M. Kolesik and J. V. Moloney. Nonlinear optical pulse propagation simulation: From Maxwell's to unidirectional equations. *Phys. Rev. E*, 70(3):036604, 2004.

[23] G. Genty, P. Kinsler, B. Kibler, and J. M. Dudley. Nonlinear envelope equation modeling of sub-cycle dynamics and harmonic generation in nonlinear waveguides. *Opt. Express*, 15(9):5382–5387, 2007.

[24] P. Kinsler. Optical pulse propagation with minimal approximations. *Phys. Rev. A*, 81(1):013819, January 2010.

[25] F. Biancalana, D. V. Skryabin, and P. St. J. Russell. Four-wave mixing instabilities in photonic-crystal and tapered fibers. *Phys. Rev. E*, 68(4):046603, October 2003.

[26] A. M. Zheltikov. Microstructure optical fibers for a new generation of fiber-optic sources and converters of light pulses. *Usp. Fiz. Nauk*, 177(7):737–762, 2007.

[27] S. Pitois and G. Millot. Experimental observation of a new modulational instability spectral window induced by fourth-order dispersion in a normally dispersive single-mode optical fiber. *Opt. Commun.*, 226(1–6):415–422, October 2003.

[28] J. D. Harvey, R. Leonhardt, S. Coen, G. K. L. Wong, J. C. Knight, W. J. Wadsworth, and P. St. J. Russell. Scalar modulation instability in the normal dispersion regime by use of a photonic crystal fiber. *Opt. Lett.*, 28(22):2225–2227, November 2003.

[29] W. H. Reeves, D. V. Skryabin, F. Biancalana, J. C. Knight, P. St. J. Russell, F. G. Omenetto, A. Efimov, and A. J. Taylor. Transformation and control of ultra-short pulses in dispersion-engineered photonic crystal fibres. *Nature*, 424(6948):511–515, July 2003.

[30] G. K. L. Wong, A. Y. H. Chen, S. G. Murdoch, R. Leonhardt, J. D. Harvey, N. Y. Joly, J. C. Knight, W. J. Wadsworth, and P. St. J. Russell. Continuous-wave tunable optical parametric generation in a photonic-crystal fiber. *J. Opt. Soc. Am. B*, 22(11):2505–2511, November 2005.

[31] A. Y. H. Chen, G. K. L. Wong, S. G. Murdoch, R. Leonhardt, J. D. Harvey, J. C. Knight, W. J. Wadsworth, and P. St. J. Russell. Widely tunable optical parametric generation in a photonic crystal fiber. *Opt. Lett.*, 30(7):762–764, April 2005.

[32] G. Rousseaux, C. Mathis, P. Maïssa, T. G. Philbin, and U. Leonhardt. Observation of negative-frequency waves in a water tank: a classical analogue to the Hawking effect? *New J. Phys.*, 10(5):053015, May 2008.

[33] G. Rousseaux, P. Maïssa, C. Mathis, P. Coullet, T. G. Philbin, and U. Leonhardt. Horizon effects with surface waves on moving water. *New Journal of Physics*, 12(9):095018, September 2010.

[34] L. D. Landau and E. M. Lifshitz. *The Classical Theory of Fields*. Pergamon, 4 edition, 1975.

[35] N. N. Rosanov, N. V. Vysotina, and A. N. Shatsev. Forward light reflection from a moving inhomogeneity. *JETP Lett.*, 93(6):308–312, May 2011.

[36] T. G. Philbin, C. Kuklewicz, S. Robertson, S. Hill, F. Konig, and U. Leonhardt. Fiber-optical analog of the event horizon. *Science*, 319(5868):1367–1370, 2008.

[37] D. Bermudez and U. Leonhardt. Hawking spectrum for a fiber-optical analog of the event horizon. *Phys. Rev. A*, 93(5):053820, May 2016.

[38] N. Akhmediev and M. Karlsson. Cherenkov radiation emitted by solitons in optical fibers. *Phys. Rev. A*, 51(3):2602–2607, March 1995.

[39] E. Rubino, J. McLenaghan, S. C. Kehr, F. Belgiorno, D. Townsend, S. Rohr, C. E. Kuklewicz, U. Leonhardt, F. König, and D. Faccio. Negative-frequency resonant radiation. *Phys. Rev. Lett.*, 108(25):253901, June 2012.

[40] M. Conforti, A. Marini, D. Faccio, and F. Biancalana. Negative frequencies get real: a missing puzzle piece in nonlinear optics. arXiv:1305.5264, May 2013.

[41] M. Conforti, A. Marini, T. X. Tran, D. Faccio, and F. Biancalana. Interaction between optical fields and their conjugates in nonlinear media. *Opt. Express*, 21(25):31239–31252, December 2013.

[42] C. R. Loures, A. Armaroli, and F. Biancalana. Contribution of third-harmonic and negative-frequency polarization fields to self-phase modulation in nonlinear media. *Opt. Lett.*, 40(4):613–616, February 2015.

[43] L. D. Landau, E. M. Lifshitz, and L. P. Pitaevskii. *Electrodynamics of Continuous Media*. Elsevier, New York, 2 edition, 1984.

[44] G. P. Agrawal. *Nonlinear Fiber Optics*. Academic, New York, 4 edition, 2007.

[45] M. Bass, E. W. Van Stryland, D. R. Williams, and W. L. Wolfe, editors. *Handbook of Optics*, volume 1. McGRAW-HILL, 2 edition, 1995.